First Results from the 3-D Near Infrared Imaging Array Spectrometer

N. Thatte, L. Weitzel, M. Cameron, L. Tacconi-Garman, H. Kroker A. Krabbe and R. Genzel

(Max Planck Institut für extraterrestrische Physik, Munich, Germany)

ABSTRACT

We present the first astronomical results from the New 3D Near Infrared Imaging Array Spectrometer. These include K band (1.95 to 2.45 μm) spectra and images of nearby starburst galaxies and active galactic nuclei with a spectral resolution of 1000. A special image slicer allows simultaneous spectra and imaging of an 8 arc second field of view. The background limited performance achieved by this instrument represents an order of magnitude reduction in integration time over existing near infrared cameras and spectrometers. In addition, subtraction of atmospheric OH lines may be performed with far higher accuracy.

We discuss the data reconstruction procedure, with special emphasis on flat fielding and calibration of the detector. This is complicated by the scrambled image format, which results in adjacent image pixels being widely separated on the detector. Small non linearities of the optical elements must also be dealt with carefully. We also discuss future improvements to instrument performance, including a low order adaptive optics system for compensating atmospheric turbulence.

1. INTRODUCTION

The 3D Near Infrared Imaging Spectrograph[1] developed by the Infrared Group at the Max Planck Institut für extraterrestrische Physik is a unique instrument capable of simultaneous spectroscopy and imaging in the K band (1.95 to 2.45 μm). This unique ability provides an order of magnitude reduction in integration time compared to other contemporary instruments, such as FAST[2] and IRSPEC[3].

3D had its first observing run at the 3.5 m telescope at Calar Alto in December 1993. The run was very successful, yielding data on a number of astronomical sources. In the following sections, we describe the design of the instrument, and illustrate its working principle. The data analysis for 3D turned out to be somewhat more complex than we had first imagined – Section 3 outlines why this was the case and details our data analysis procedure. Some prototype astronomical results are presented in Section 4. Section 5 discusses the Rapid Off-Axis GUider Experiment (ROGUE), a proposed system to enhance the performance of the instrument by correcting for atmospheric *seeing* effects.

2. INSTRUMENT DESIGN

2.1 Motivation

The information available from any astronomical source is three dimensional in form – two spatial dimensions in the plane of the sky and a spectral (or wavelength) dimension along the line of sight. With most instruments, only two of these three dimensions are *simultaneously* accessible to the astronomer. A camera (often equipped with a narrow wavelength filter) has access to the two spatial dimensions. By scanning the central frequency of the filter, it is possible to build up the wavelength information over a period of time. In contrast, a long slit spectrometer allows the astronomer to capture one spatial dimension (along the slit) and the spectral dimension simultaneously on a square detector array. The three dimensional information set (the data cube) can be built up by scanning the long slit across the sky as a function of time.

3D is the first instrument at near infrared wavelengths capable of obtaining information in all three dimensions simultaneously. This unique capability obviates the need to make several scans to build up the data cube, resulting in much shorter observing times. The background limited performance of the instrument allows long

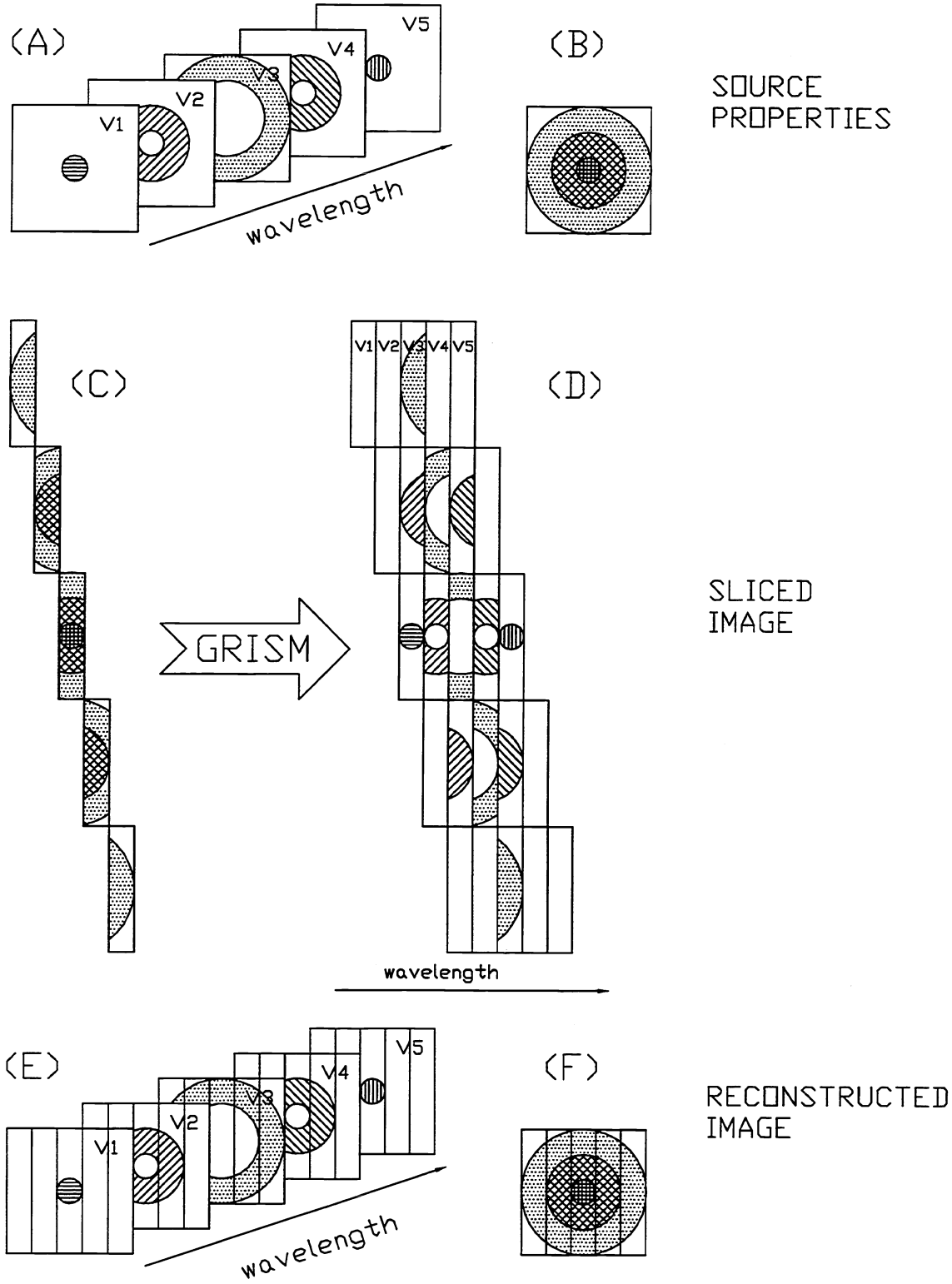

Figure 1: Principle of the 3D Image Slicer

periods of integration on a single astronomical source, allowing 3D to image fainter sources within a given time period, as compared to other instruments.

2.2 Working Principle

The capability of simultaneous imaging and spectroscopy is made possible via a specially constructed image slicer. The principle of the image slicer is explained in figure 1. Consider an emission line observed in an astronomical source which is an expanding shell, e.g. a supernova remnant. The source structure is shown in (A), where we denote the spectral dimension by showing five cuts at different wavelengths. Each wavelength corresponds to a distinct velocity along the line of sight, a consequence of the Doppler effect. In this example, V_3 is the systemic velocity of the source, while V_1 and V_5 are the two velocity extremes. The information from the various spectral cuts is superimposed spatially. The source, as viewed by a broad band detector, would appear as shown in (B).

The image slicer splits the source image into several vertical slices. Five slices are shown in the schematic figure, the actual instrument has 16 slices. These slices are then realigned in one dimension so that the resulting image is as shown in (C). Note that all the velocity information is still contained within each slice. It is also important to observe that the slices are not aligned one below the other, but each slice is displaced with respect to its neighbor by one slice width. The resulting image, (C), resembles the slit of a long slit spectrograph. This is then passed through the dispersing element (a grism) to yield the image shown in (D). The grism smears the image of each slice in the wavelength dimension. In our schematic, each slice now corresponds to five images, one for each wavelength (or velocity) cut. The output of the grism, (D), is imaged onto a square detector array. The actual instrument uses a 256×256 detector array, yielding 256 spectral data points for each spatial pixel. There are 256 spatial pixels, with 16 pixels in each of 16 slices.

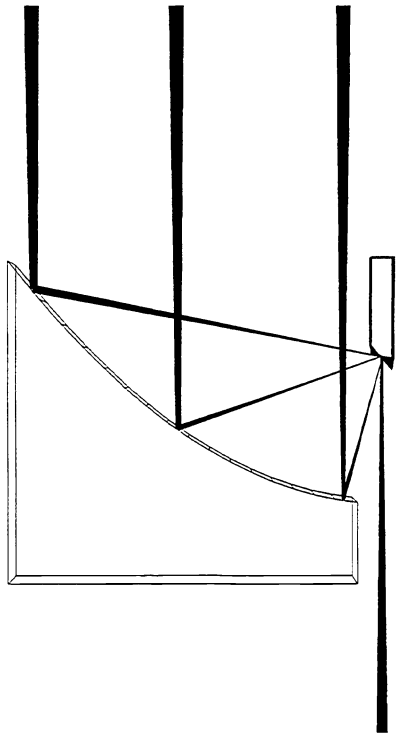

Figure 2: View of the 3D Image Slicer, showing the optical ray paths

The detected signal is read by the control computer, which then undertakes the job of reconstructing the original data cube. In principle, this is achieved by a simple re-alignment of the various image slices, as shown in (E). For example, the cut at velocity V_1 is built up using the leftmost spectral parts of each image slice. The same technique is used for the the other images. The image in (E) is an exact replica of the source in (A), as desired. If required, the data from the various wavelength cuts can be added together to yield a composite image of the source spanning the whole spectral range. Such a reconstruction is shown in (F).

2.3 The Image Slicer

Figure 2 shows a top view of the image slicer. The slicer is composed of two sets of mirrors. The first (and smaller) set of mirrors is located at the focal plane of the telescope beam. The input beam is split into 16 slices by these mirrors. The light from each slice is redirected at a slightly different angle to a second set of mirrors, which form a section of a parabola. The first mirror set is located at the focus of this parabola. After redirection by the second set of mirrors, the beam emerges parallel to itself, split into 16 slices which are lined up end to end. All the reflecting surfaces are located perpendicular to the plane of figure 2. As a result, the realigned image retains its original form perpendicular to the slicer plane. This results in the offset between slices depicted in figure 1C.

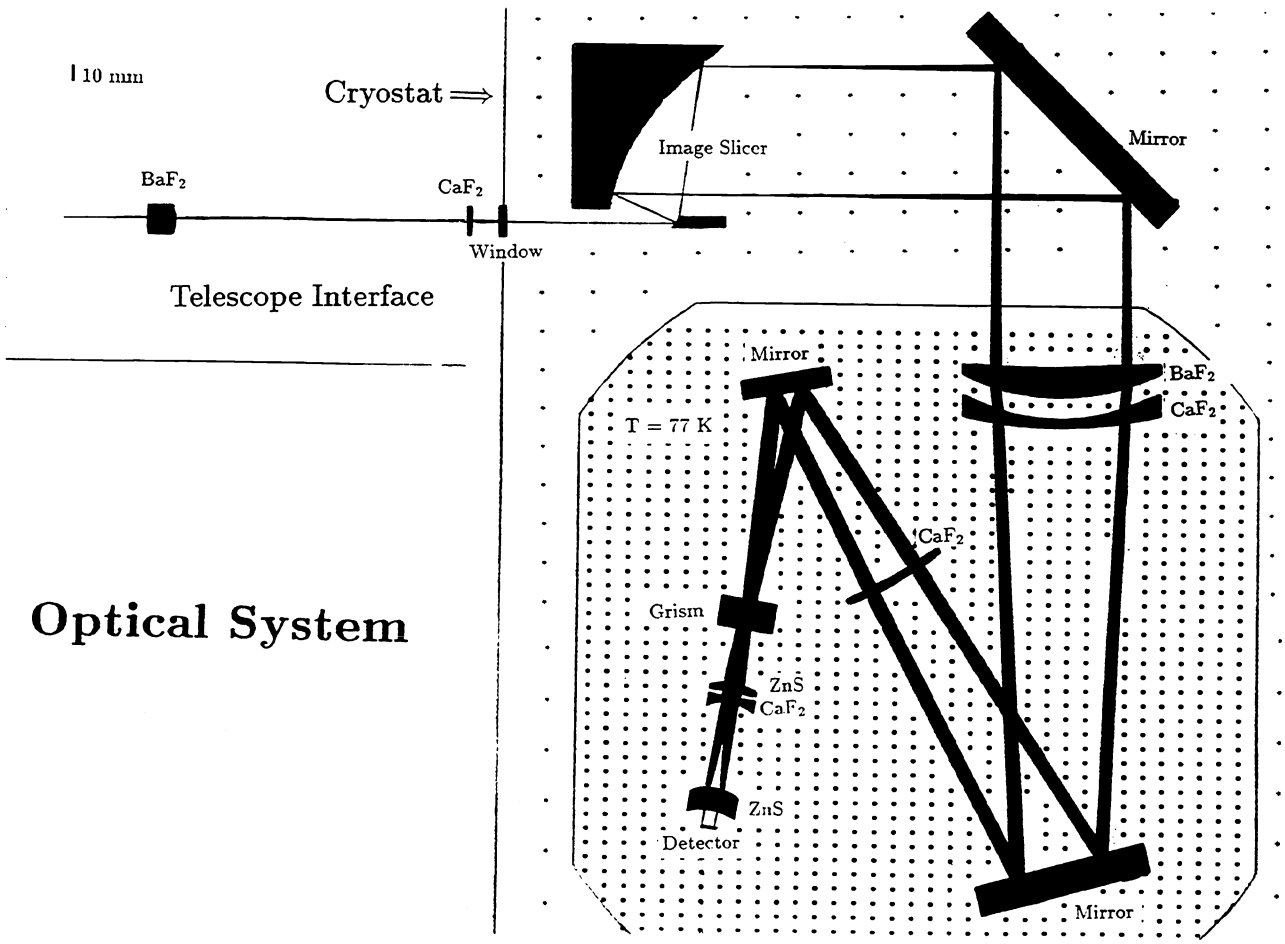

Figure 3: Layout of the 3D dewar

2.4 Optical Design

The optical layout of the instrument is shown in figure 3. Thermal emission from components at room temperature contributes a substantial background at wavelengths between 1.95 and 2.45 μm. The entire optical assembly is cooled to 77 K to eliminate the thermal background. The light from the telescope enters the cryostat through a small window. The first optical element, the image slicer, is located at the focal plane of the telescope. The diverging beam from the image slicer passes through collimating lenses onto the grism. The collimating lens forms an image of the telescope entrance pupil (often the secondary mirror) onto the grism. In other words, each point in the image creates the *same* blur circle at the grism. An appropriately sized baffle placed at this point further reduces background contamination. The dispersed beam is re-imaged onto the NICMOS III detector array.

3. DATA RECONSTRUCTION

The output of the 256×256 array detector resembles that of a long slit spectrograph. The y axis represents wavelength, while the units for the x axis are arc seconds on the sky. In principle, it is easy to reorganize the information from the array detector to create a data cube, with 2 spatial dimensions, and 1 wavelength dimension. For the actual instrument, the reconstruction is complicated by a number of practical issues.

3.1 Spectral Re-projection

As shown in figure 1, the long slit created by the slicer is not aligned with the x and y axes of the detector. Successive slit images are shifted by 1 pixel in the wavelength direction. In other words, a fixed y co-ordinate at the detector does not correspond to a single wavelength. The first step in the data reconstruction (after dark current subtraction and dead pixel blanking) is to realign the wavelength axes for the various columns. It is also necessary to establish an absolute wavelength scale for each detector pixel, using a calibration spectrum from a neon lamp.

The re-alignment and absolute wavelength calibration are complicated by the presence of a slight non-linearity in the grism dispersion curve. This results in a non-uniform wavelength scale for each column. Although the non-linearity is only of the order of 1%, this corresponds to 2.56 pixels over a 256 pixel range. Further, the non-linearity is not the same for all columns of the detector array.

A comparison of the actual spectrum of a neon lamp with a theoretical neon spectrum is used to generate a calibration image. Each pixel in the calibration image has a value denoting its wavelength in microns. For each column of the detector, we perform a cross-correlation between the theoretical spectrum and the actual spectrum. Prior to cross-correlation, the non-linear correction factor for that column is applied to the theoretical neon spectrum. The cross-correlation yields the relative shift between the theoretical and actual spectra, allowing us to determine the absolute wavelength for each pixel in that column.

Having established an absolute wavelength calibration, it is possible to realign the columns of each image such that all pixels with a given y co-ordinate have the same wavelength associated with them. This is achieved by interpolating the data in each column of the original image. The desired interpolation wavelength for each pixel is obtained from the calibration image. The interpolation is performed by fitting a polynomial to a set of data points centered at the desired wavelength. The number of data points and the order of the polynomial fit are parameters chosen by the user. A consequence of the grism non-linearity is that the interpolation points are not equally spaced, preventing the use of faster linear interpolation techniques. The realigned image is not square, having approximately 272 rows and 256 columns, although each column has only 256 valid pixels. Extra pixels introduced by the re-alignment procedure are set to zero value.

3.2 Spatial Re-projection

Each image slice is designed to span exactly 16 detector pixels, 16 such slices constituting the complete sky image. Practical limitations of alignment and fabrication of the optical elements leads to a total image extent

of 252.8 pixels, instead of the theoretical 256 pixels. Non-linearities in the construction of the image slicer also introduce variations in the number of detector pixels spanned by each image slice.

In order to reconstruct the two dimensional image from the 16 image slices, it is necessary to determine the relative shift between the center points of the slices. An exposure is made while moving a star across the entire field of view in a north-south direction. The image slices are then aligned so as to yield a stellar image smeared precisely in a vertical direction, allowing us to determine the relative shift of each slice to a fraction of a pixel. The amount of the shift is non-integer, making it necessary to re-sample the data from each spatial slice. The re-sampling is carried out using FFT techniques, since, unlike the spectral dimension, the spatial data is adequately sampled. The edges of each slice often contain pixels receiving light from two spatial slices. These pixels do not contain any useful information, and are discarded.

3.3 Flat Fielding

The unique nature of 3D implies that the source used for flat fielding must be both spatially and spectrally flat. As no source satisfies both these constraints simultaneously, the flat fielding is carried out in two stages, first in the spatial and then in the spectral dimension.

The spatial flat field is obtained from an image of blank sky (sky flat) or from an image of the telescope dome (dome flat). The image is re-projected spatially and spectrally as described in the previous sections. Each spatial slice of the resulting data cube represents an image of blank sky. As the source has no spatial features, all variations amongst the 256 pixels which make up a spatial slice are attributable to irregularities in the detector response. Each slice is separately normalized to yield the desired spatial flat field.

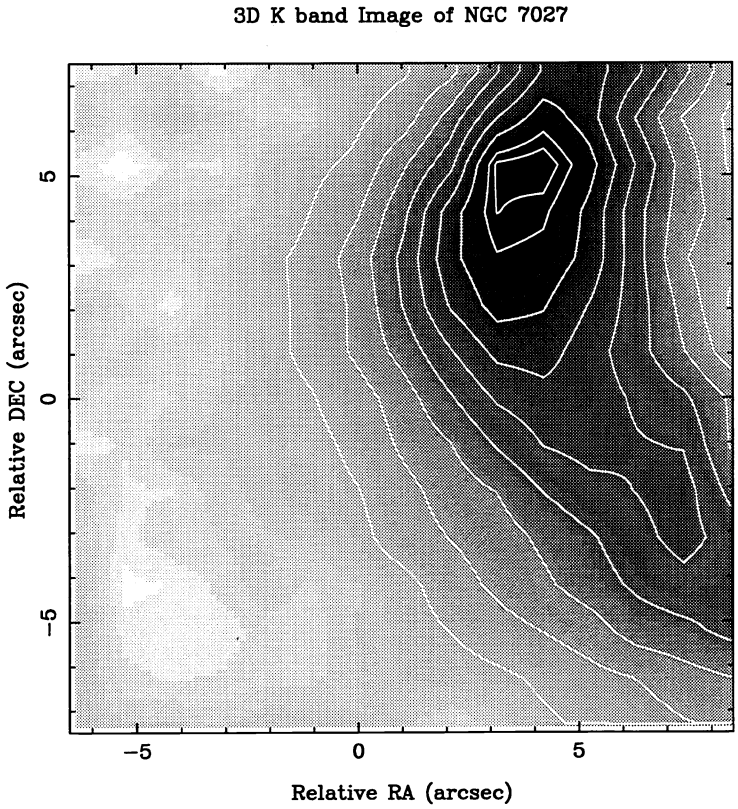

Figure 4: Composite K band image of the planetary nebula NGC 7027, observed with 3D

The spectral flat field is obtained in a similar manner. The template source is a Nernst-glower whose spectrum approximates that of a black body. As the template source is not spectrally flat, its spectral shape is obtained by comparison with a black body of known temperature in the laboratory. This spectral shape is compared with the spectral response obtained for each spatial pixel of the re-projected image, to yield the spectral flat field for each pixel. This is combined with the spatial flat field to yield the overall detector flat field.

We would like to note that an accurate knowledge of the spectral shape of the Nernst-glower is not critical to the data reduction process. In most cases, the observed spectrum of the source under study is divided by the spectrum of a template star, in order to remove any spectral features introduced by the atmosphere. As a result, absolute spectral flatness of the detector is not required, a relative flat field is sufficient. The final data cube may be collapsed in the velocity (or spectral) dimension to yield a composite K band image of the astronomical source.

4. PRELIMINARY RESULTS

Figures 4 and 5 show some preliminary astronomical results from the first observing run at the 3.5 meter telescope at Calar Alto in December 1993. Figure 4 shows a grey scale representation of a composite K band image of the planetary nebula NGC 7027. The image shows a part of the nebular ring. Figure 5 shows a spectrum centered at the emission peak of figure 4. The prominent K band emission lines are marked[4]. These two figures show the simultaneous imaging and spectroscopy capabilities of 3D. These results represent only a preliminary calibration of the data, as all the data calibration and analysis software is not yet in place.

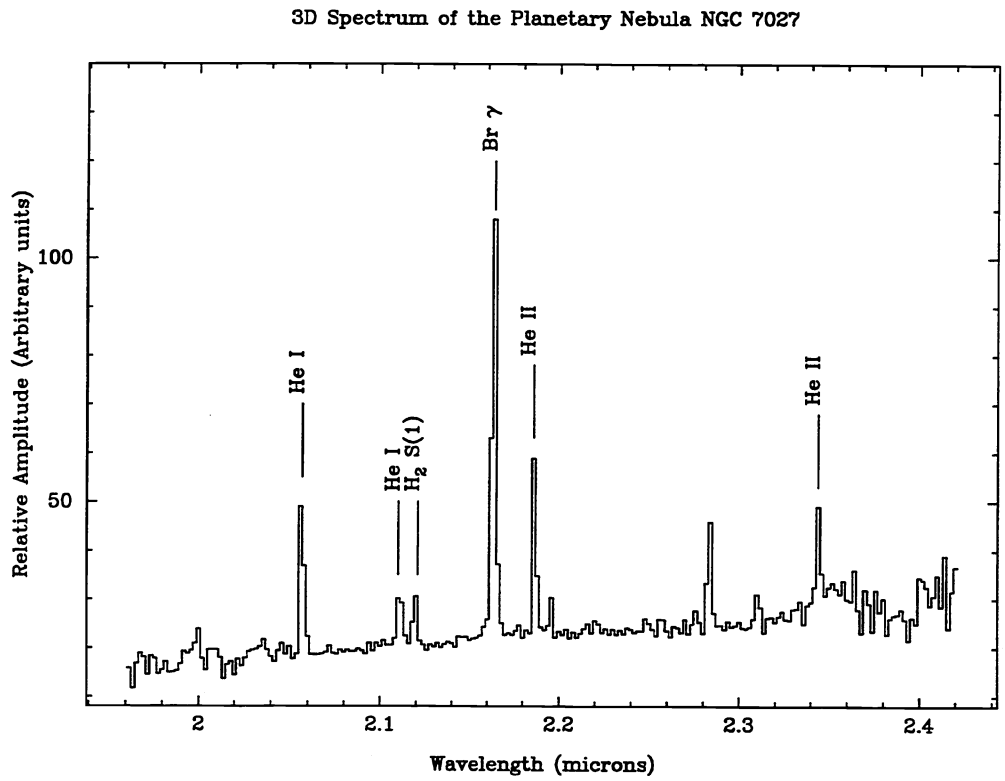

Figure 5: Spectrum of the planetary nebula NGC 7027, observed with 3D

5. FUTURE IMPROVEMENTS

Several improvements to 3D are planned in the near future. An H band (1.4 to 1.8 μm) grism will be added to the instrument, allowing imaging in both the H and K atmospheric windows. A higher resolution grism

in the K band is also planned, improving the spectral resolution ($\lambda/\delta\lambda$) to 3000, from it's present value of 1000.

5.1 Atmospheric Seeing Correction

Ground based imaging in the near infrared does not achieve diffraction limited performance due to turbulence in the atmosphere. Atmospheric fluctuations affecting K band imaging have a time constant of approximately 50 milliseconds (20 Hz). The first order effect of the atmospheric fluctuations, termed *seeing*, is to move to the image of the astronomical source by small amounts. This rapid image motion results in a blurred image, whose size is larger than the diffraction limit of the telescope in use. The size of the image of a point source, such as a star, is often about 1 arc second at good astronomical sites, increasing to 2 arc seconds on nights with bad seeing.

The degradation resulting from atmospheric turbulence can be dramatically reduced by *speckle imaging*. This involves rapid imaging, at a frequency equal to that of the atmospheric turbulence. The images are then co-added by a simple Shift And Add technique, in which a bright point source in the field of view is used to align the various images with respect to each other. The complex image slicing done by 3D makes it very difficult to implement such a shift and add technique with 3D. Instead, it is necessary to correct for atmospheric image motion before the light enters 3D. We are currently building ROGUE (Rapid Off-axis GUider Experiment) for this purpose.

ROGUE is a low order adaptive optics system, whose purpose is to correct for image motion in two orthogonal directions (tip-tilt correction). As 3D operates in the near infrared, ROGUE uses visible light (450 to 900 nm) to determine the amount of image motion introduced by the atmosphere. This is done using a quadrant detector composed of four Avalanche Photo Diodes (APDs). The image of guide star located close (within 2 arc minutes) to the object of interest is split into four quadrants. An APD is used to count the number of photons received in each quadrant. An image motion results in an imbalance in the number of counts in the four quadrants. This difference signal is used to drive a piezo controlled plane mirror so as to compensate for the image motion. In this manner, a factor of 2 improvement in resolution may be easily achieved.

The challenge in designing ROGUE is to correct for atmospheric seeing using very faint guide stars. The correction determined by the quadrant APD system is valid only in near vicinity of the reference object. Hence, it is necessary to find a guide star close to the object of interest being imaged with 3D. The chances of finding such a guide star improve dramatically if one can use relatively faint stars. ROGUE is being designed to use stars brighter than 19th magnitude at a 3.6 meter telescope. This results in very few photons in each sampling interval, requiring the system to have a very high efficiency. A high transmission is also required in the near infrared, as we would like to image faint objects with 3D. ROGUE is scheduled for its first observing run at the ESO 2.2 meter telescope at La Silla in July 1994.

REFERENCES

1. L. Weitzel, M. Cameron, S. Drapatz, R. Genzel and A. Krabbe, *in Proceedings of the Los Angeles Conference* on "Infrared Astronomy with Arrays: The Next Generation", held at UCLA, July 1993. *Experimental Astronomy*, editors Ian S. McLean and George Brims, (Dordrecht:Kluwer) in press.

2. A. Krabbe, V. Rotaciuc, J. W. V. Storey, M. Cameron, M. Blietz, S. Drapatz, R. Hofmann, G. Sämann and R. Genzel, *Publications of the Astronomical Society of the Pacific*, Vol 105, p. 1472, 1993.

3. R. Gredel and A. F. M. Moorwood, *European Southern Observatory Operating Manual*, No. 10, 1991.

4. T. R. Geballe, M. G. Burton and R. Isaacman, *Monthly Notices of the Royal Astronomical Society*, Vol. 253, p. 75, 1991.